

Constraining QCD transport coefficients in hadron colliders

Akihiko Monnai^{1,*}

¹KEK Theory Center, Institute of Particle and Nuclear Studies, High Energy Accelerator Research Organization (KEK), 1-1, Ooho, Tsukuba, Ibaraki 305-0801, Japan

Abstract. We review the phenomenology of relativistic nuclear collisions in the light of ultra-high energy cosmic ray physics. A novel phase of quantum chromodynamics called quark-gluon plasma is expected to appear in nuclear collisions at high energies. The produced hot matter is found to be well-described as a relativistic fluid with small viscosity. We show that the transport coefficient can be quantitatively extracted by comparing theoretical estimations of viscous hydrodynamic models to experimental data.

1 Introduction

The physics of relativistic nuclear collisions and that of ultra-high energy cosmic ray (UHECR) events share a common ground since the former has its roots in the study of multi-particle production introduced in the context of cosmic ray analyses [1]. Experimental nucleus-nucleus collisions were first achieved at Bevalac in Lawrence Berkeley National Laboratory in 1971. Following construction of upgraded facilities, the beam energy has been increased by orders of magnitude since then; the top center-of-mass energy of proton-proton collisions at the CERN Large Hadron Collider (LHC) is now $\sqrt{s} = 13$ TeV. While this is still lower than the typical energy scale of UHECR, which is about $\sqrt{s} = 300$ TeV, we have in collider experiments the unique opportunity to perform detailed analyses of the nuclear collision events under a controlled environment.

An interesting observation arise by comparing proton-proton and heavy ion – such as gold (Au) or lead (Pb) nuclei – collisions. The BNL Relativistic Heavy Ion Collider (RHIC) was the first to observe clear evidences of the creation of quark-gluon plasma (QGP) in Au-Au collisions at $\sqrt{s_{NN}} = 200$ GeV [2–5]. The QGP is a high-temperature phase of quantum chromodynamics (QCD) where quarks and gluons are deconfined from hadrons above 2 trillion degrees [6]. It has been now shown at RHIC and LHC that the QGP can be realized over various energies. The presence of the hot QCD medium has been considered to make heavy ion collisions qualitatively different from the naïve scaling of proton-proton collisions. Recent experimental results also suggest that a hot medium could be produced in the collisions of lighter nuclei at top beam energies. This implies that the insight obtained though QCD collider experiments is also relevant to the analyses of UHECR, where light nuclei collide at very high energies.

One evidence for the existence of the quark fluid is the large *elliptic flow* [7, 8] observed in off-central collisions. Elliptic flow can be understood as the second harmonics v_2 of the Fourier series expansion of azimuthal momentum distribution, which denotes the momentum anisotropy of the particle yield in transverse directions, as defined in

$$\frac{dN}{d\phi} = \frac{N}{2\pi} [1 + 2v_n \cos(n\phi - n\psi_n)], \quad (1)$$

where N is the particle number, ϕ is the azimuthal momentum angle and ψ_n is the participant plane of the n -th harmonics in which the sine component is embedded. Odd-order flow harmonics, such as triangular flow v_3 , is also non-vanishing when the initial geometry is fluctuating. The heavy ion systems have little initial momentum anisotropy but it can be transferred from spatial anisotropy of the overlapping region of colliding nuclei if there is a medium and if it is strongly coupled. It is found in the experiments that the observed elliptic flow is large and it strongly reflects the spatial anisotropy. The data show an excellent agreement with the nearly-perfect fluid picture, which indicates that the QGP is strongly coupled and locally thermalized. This implies that one can use a relativistic hydrodynamic model for the effective description of the dynamical evolution of non-perturbative QCD systems. Low momentum hadrons below $p_T \sim 2$ GeV are understood to be produced mostly by the hot medium and by the decay processes of massive hadrons. Here p_T denotes the transverse momentum.

The application of relativistic hydrodynamics to the nuclear collision events dates back to the Landau model [9] albeit in the context of proton-proton collisions. The full-stopping picture of the model is later improved with the transparent picture by Bjorken [10]. In the most state-of-art hydrodynamic modeling for heavy ion collisions, the system is understood to go through several stages (Fig. 1). The colliding nuclei at relativistic energies are considered to be dominated by saturated gluons called color glass condensate [11, 12]. After the colli-

*e-mail: akihiko.monnai@kek.jp

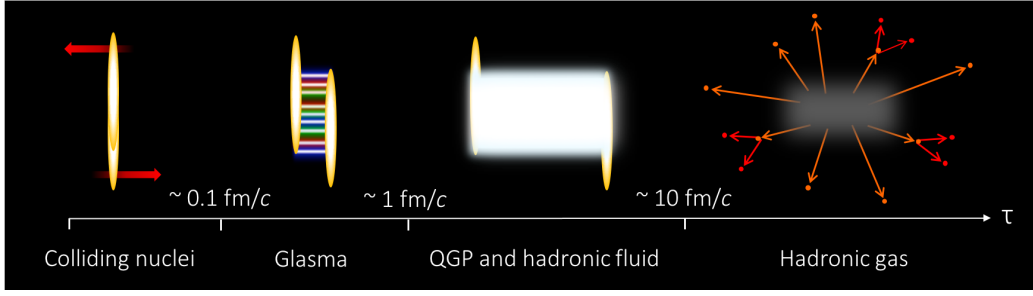


Figure 1. Schematic of the space-time evolution of a high-energy heavy ion collision.

sion, the system reaches local thermal equilibrium in less than 1 fm/c and starts to behave as a fluid with extremely small viscosity. The exact mechanism of the early thermalization is not fully understood, but it speculated that longitudinal color electric and magnetic fields are formed during the process [13]. This stage is often referred to as “glasma”, which is a combination of the terms “glass” and “plasma”. The hydrodynamic evolution remains valid until about 10 fm/c before the system cools down and hadrons decouple from thermal equilibrium. This is called freeze-out [14], which can be regarded as the “clear-up” of the heavy ion system in terms of strong interaction. The system then is described as a weakly-interacting hadronic gas until the particles reach detectors. The transport and decay processes can be described using hadronic cascade models.

2 Relativistic hydrodynamics and transport coefficients

Relativistic hydrodynamic equations of motion are given by energy-momentum and net baryon number conservation laws $\partial_\mu T^{\mu\nu} = 0$ and $\partial_\mu N_B^\mu = 0$ in inviscid systems. The energy-momentum tensor and the net baryon number current can be decomposed in terms of the hydrodynamic flow u^μ as

$$T^{\mu\nu} = (\epsilon + P)u^\mu u^\nu - P g^{\mu\nu}, \quad (2)$$

$$N_B^\mu = n_B u^\mu, \quad (3)$$

where ϵ is the energy density, P is the hydrostatic pressure and n_B is the net baryon number. $g^{\mu\nu}$ is the mostly-minus Minkowski metric. The physical properties of the fluid is characterized by the equation of state $P = P(\epsilon, n_B)$, which is a static relation between thermodynamic variables. n_B is typically small at high-energy nuclear collisions near the center of the medium since most particles are created through pair productions and thus the quantity is sometimes neglected in numerical estimations.

Off-equilibrium corrections, on the other hand, are encoded in viscosity in hydrodynamic systems. The constitutive relations among the additional macroscopic quantities are derived from the second law of thermodynamics [15]. The off-equilibrium energy-momentum tensor and

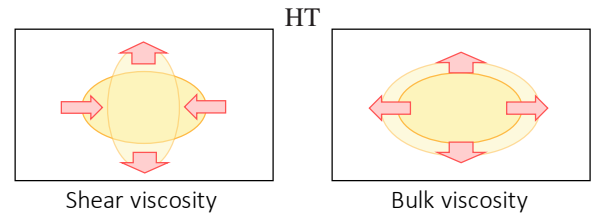


Figure 2. Schematic of the thermodynamic forces for the shear viscosity and the bulk viscosity.

net baryon number current are

$$T^{\mu\nu} = (\epsilon + P + \Pi)u^\mu u^\nu - (P + \Pi)g^{\mu\nu} + \pi^{\mu\nu}, \quad (4)$$

$$N_B^\mu = n_B u^\mu + V_B^\mu, \quad (5)$$

and the minimalistic constitutive equations for the dissipative currents can be expressed as

$$\pi^{\mu\nu} = 2\eta\partial^{(\mu}u^{\nu)} - \tau_\pi u^\rho\partial_\rho\pi^{(\mu\nu)}, \quad (6)$$

$$\Pi = -\zeta\partial_\mu u^\mu - \tau_\Pi u^\mu\partial_\mu\Pi, \quad (7)$$

where $\pi^{\mu\nu}$ is the shear stress tensor and Π is the bulk pressure. Here the flow is defined in Landau frame where it is in the direction of the energy flux. Baryon diffusion V_B^μ [16, 17] is assumed to be vanishing for simplicity. The corrections to the energy density and the baryon number density can also be kept finite [18]. The angle brackets on indices denote traceless symmetrization. The medium properties are characterized by transport coefficients; η is the shear viscosity, ζ is the bulk viscosity, τ_π and τ_Π are the relaxation times introduced in relativistic formulation of hydrodynamics for preserving causality and stability. More non-linear terms are present in a complete relativistic formulation of viscous hydrodynamics, which is later discussed. One can see in the linear response regime that the shear viscosity is the response to medium deformation and the bulk viscosity is the response to volume change (Fig. 2). The shear viscosity provides larger contribution because the bulk viscosity is small except around the QCD crossover region where the conformal condition is explicitly broken $T_\mu^\mu \neq 0$.

The equation of state can be estimated at the vanishing density using the first principle approach with the advent of lattice QCD techniques [19, 20]. The quark-hadron transition of (2+1)-flavor QCD is now known to

be crossover-type. At finite density, on the other hand, it cannot be calculated owing to the fermion sign problem. The model estimation based on chiral perturbation theory suggests that the crossover transition becomes a first-order phase transition at some finite density, implying the existence of a critical point. This is now being actively searched theoretically and experimentally.

Transport coefficients cannot be directly calculated from QCD in the strongly coupled regime. One approach to strong-coupling field theories was proposed in the context of string theory; Anti-de Sitter/conformal field theory (AdS/CFT) correspondence conjectures that the 5 dimensional AdS black hole is dual to the 4 dimensional $\mathcal{N} = 4$ super Yang-Mills theory [21]. This allows one to calculate the shear viscosity and the universal lower bound $\eta/s = 1/4\pi$ was proposed [22]. Here s is the entropy density. The value is found to be smaller than the viscosity of known matter, and this naturally attracted attention of the heavy ion community in regards to its application to QCD physics since the heavy ion collision system is experimentally suggested to be a nearly-perfect fluid. Many studies assume that η/s of QCD is constant based on the AdS/CFT conjecture, but there remains large uncertainty since QCD is not a conformal field theory. It is thus quite important to extract the temperature dependence of the QCD transport coefficients from experimental data quantitatively by comparing them to theoretical estimations.

3 Numerical analyses of heavy ion collisions

We show that the shear viscosity can be constrained from experimental data using a relativistic hydrodynamic model for heavy ion collisions as done by Denicol, Monnai and Schenke [23]. Comparison between the experimental data and the results of numerical simulation with model viscous coefficients allows one to indirectly extract the information of QCD transport coefficients from the data of relativistic nuclear collisions. A state-of-art relativistic viscous hydrodynamic equations [24, 25] are solved using a (3+1)-dimensional numerical hydrodynamic model [26].

An observable sensitive to the viscosity is elliptic flow v_2 because viscous correction is the deviation from local thermal equilibrium. v_2 quantifies how strongly the system is coupled, *i.e.*, how close the system is to local equilibrium. Shear viscous corrections are known to make the azimuthal momentum anisotropy smaller, reducing v_2 . To investigate the temperature dependence of the transport coefficient, the rapidity dependence of elliptic flow is used. Here the rapidity is a measure of the longitudinal momentum p_z defined as

$$y = \frac{1}{2} \log \frac{E + p_z}{E - p_z}. \quad (8)$$

The QCD medium is typically hot near the central region and becomes colder towards the peripheral regions in the space-time coordinates, and this is reflected in momentum space. Thus, the transport coefficients at higher temperature is expected to be probed in mid-rapidity regions and

that at lower temperature is in forward rapidity regions, given that one knows the temperature dependence of the equation of state.

One needs precise initial conditions that reflect the geometrical properties of heavy ion collisions. One conventional choice for the transverse coordinate space distributions is given by the Glauber model. In the Monte-Carlo version of the model, nucleons are distributed according to a Woods-Saxon function. Sub-collisions of nucleons are assumed when the distance between two nucleons from different nuclei is smaller than $\sqrt{\sigma_{nn}/\pi}$ where σ_{nn} is the inelastic nucleon-nucleon cross section.

The longitudinal profile of the initial condition is required to estimate the rapidity distribution. The Glauber-Lexus model [27] is a full three-dimensional model constructed by combining the aforementioned model to the Lexus picture [28]. Valence quarks are considered instead of nucleons to take account of the nucleon structure. Valence quark parton distribution functions are used for constructing initial parton rapidity distribution. For each sub-collision, longitudinal momentum is exchanged via the probability

$$Q(y - y_T, y_P - y_T, y - y_P) = \lambda \frac{\cosh(y - y_T)}{\sinh(y_P - y_T)} + (1 - \lambda)\delta(y - y_P), \quad (9)$$

where y_P is the rapidity of the projectile parton before the sub-collision, y_T is the rapidity of the target parton and λ is the parameter controlling the stopping power. This is a most straight-forward extension of the two-dimensional Monte-Carlo Glauber model.

The equation of state is based on lattice QCD calculations. Although the net baryon number has little effect in high-energy collisions as mentioned earlier, they can still be introduced to the model for theoretical completeness. The equation of state at finite density is constructed [27] by matching the Taylor expansion results of lattice QCD [19, 29] to the hadron resonance gas model, which exhibits excellent agreement with the lattice QCD estimations at vanishing density, as

$$\frac{P}{T^4} = \frac{1}{2} \left[1 - \tanh \left(\frac{T - T_c(\mu_B)}{\Delta T} \right) \right] \frac{P_{\text{HRS}}(T, \mu_B)}{T^4} + \frac{1}{2} \left[1 + \tanh \left(\frac{T - T_c(\mu_B)}{\Delta T} \right) \right] \frac{P_{\text{lat}}(T_s, \mu_B)}{T_s^4}. \quad (10)$$

Here the connecting temperature is $T_c(\mu_B) = 0.166 \text{ GeV} - 0.4 \times (0.139 \text{ GeV}^{-1} \mu_B^2 + 0.053 \text{ GeV}^{-3} \mu_B^4)$. This is motivated by the chemical freeze-out curvature [30]. The connecting width is $\Delta T = 0.1 \times T_c(0)$. The temperature shift $T_s = T + 0.4 \times [T_c(0) - T_c(\mu_B)]$ is introduced to ensure thermodynamic consistency at large μ_B . It has limited effect in the current analyses since μ_B is small. This approach ensures that the energy-momentum and net baryon number are conserved when fluids are converted into hadrons using relativistic kinetic theory [14] at thermal freeze-out. The criterion for the freeze-out here is the energy density of $0.1 \text{ GeV}/\text{fm}^3$.

Several parameterizations are prepared for the model of the shear viscosity. The entropy density is replaced by

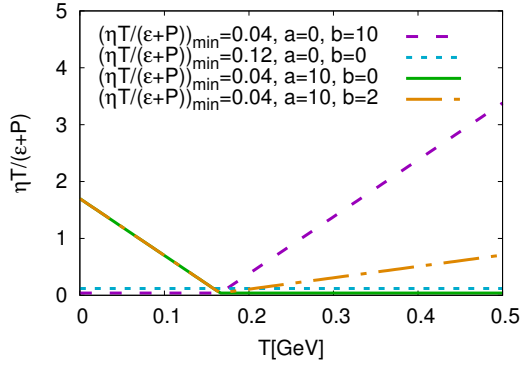


Figure 3. Parameterizations of the shear viscous coefficient. The figure is from Ref. [23].

the enthalpy over temperature at finite density:

$$\begin{aligned}
 (\eta T / (\epsilon + P))(T) &= (\eta T / (\epsilon + P))_{\min} \\
 &+ a \times (T_c - T)\theta(T_c - T) \\
 &+ b \times (T - T_c)\theta(T - T_c), \quad (11)
 \end{aligned}$$

where a and b are parameters. The functional form has a minimum around T_c for positive values of a and b . This behavior [31] is partly motivated by the fact that perturbative QCD calculations indicate that it rises in the QGP phase [32] and that chiral perturbation theory implies that it decreases in the hadronic phase [33]. $\eta T / (\epsilon + P)$ as a function of the temperature for several choices of the parameters are plotted in Fig. 3: $(\eta T / (\epsilon + P))_{\min} = 0.04$ with $(a, b) = (0, 10)$, $(10, 0)$ and $(10, 2)$, and $(\eta T / (\epsilon + P))_{\min} = 0.12$ with $(a, b) = (0, 0)$. Since the focus is on the shear viscosity, the bulk viscosity is simply parametrized as in Ref [34]. Variation of the bulk viscosity can be found, for example, in Ref. [35]. The relaxation times and other higher-order transport coefficients are estimated using the Boltzmann equation in the conformal limit.

For numerical estimations, Au-Au collisions at $\sqrt{s_{NN}} = 200$ GeV are considered. Here the pseudo-rapidity

$$\eta_p = \frac{1}{2} \log \frac{|\mathbf{p}| + p_z}{|\mathbf{p}| - p_z}, \quad (12)$$

is defined for comparison to experimental data. The quantity reduces to the rapidity in the massless limit and does not require particle identification. The centrality is defined as the groups of events per multiplicity ordered from the most central to peripheral collisions. The initial conditions are tuned to reproduce the charged particle rapidity distribution for each parameter set of the shear viscosity.

The pseudo-rapidity dependence of the elliptic flow v_2 of charged hadrons are plotted with PHOBOS data [36, 37] for 0-40% centrality events in Fig. 4. The flow harmonics $v_n(\eta_p)$ here is calculated using the event average

$$v_n\{2\}(\eta_p) = \frac{\langle v_n v_n(\eta_p) \cos[n(\psi_n - \psi_n(\eta_p))] \rangle}{\sqrt{\langle v_n^2 \rangle}}. \quad (13)$$

One can see that large hadronic viscosity and small QGP viscosity are favored by the experimental data. The one

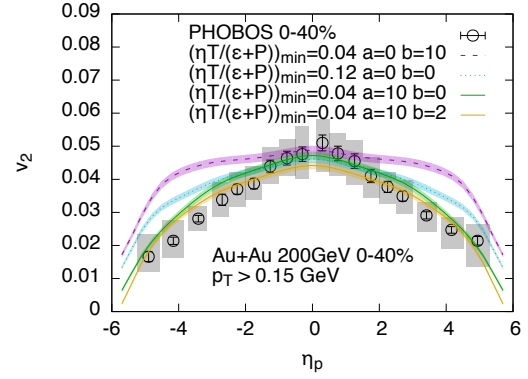


Figure 4. The elliptic flow v_2 as a function of the pseudo-rapidity. The data is from the PHOBOS [36, 37]. The figure is from Ref. [23].

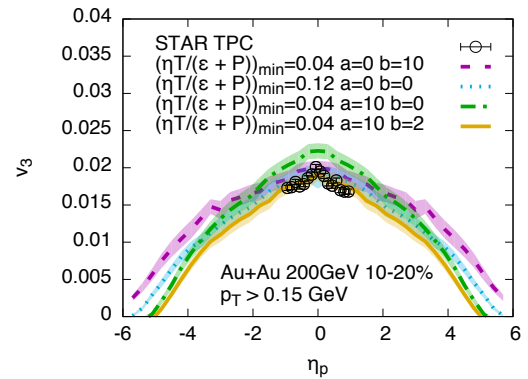


Figure 5. The triangular flow v_3 as a function of the pseudo-rapidity. The data is from the STAR [39]. The figure is from Ref. [38].

with large hadronic viscosity ($a = 0, b = 10$) and the constant viscosity ($a = b = 0$) do not describe the data at forward rapidity well. The quick drop of $v_2(\eta_p)$ in the large η_p region is induced in the large hadronic viscosity scenarios because of the increased shear viscous correction in colder regions. It should be noted that the minimum value of shear viscosity near T_c , $(\eta T / (\epsilon + P))_{\min} = 0.04$, is much smaller than that of the AdS/CFT conjecture $\eta/s = 1/4\pi \sim 0.08$. Here the finite density effect is small, *i.e.*, $(\epsilon + P)/T$ can be replaced with s at the collision energy of interest. The result implies that one should be careful about the applicability of the AdS/CFT correspondence to QCD systems.

One can also calculate the triangular flow $v_3(\eta_p)$, which is the third flow harmonics [38]. The quantity is non-vanishing for event-by-event simulations of hydrodynamics because of the initial fluctuations in the geometry. The pseudo-rapidity dependence of v_3 is shown in Fig. 5 for 10-20% centrality events. The STAR data is plotted for comparison [39]. There are few data at forward rapidity for the triangular flow, but the numerical result is

still consistent for the scenario where hadronic viscosity is large and QGP viscosity is small but slowing increasing.

4 Summary and outlook

We have studied collective properties of the hot QCD matter in relativistic nuclear collisions, which can be relevant in the analyses of ultra-high energy cosmic ray events. The quark-gluon plasma can be produced in relativistic heavy ion collisions, and it is found to behave as a relativistic fluid with extremely small but non-vanishing viscosity. Numerical estimations of relativistic viscous hydrodynamic models allow one to constrain the QCD shear viscosity, a quantity which is difficult to estimate in the first principle calculation, using the rapidity dependence of the elliptic and the triangular flow, v_2 and v_3 . The experimental data are found to favor large hadronic viscosity and small QGP viscosity. The minimum of the temperature dependent shear viscosity can be smaller than the universal lower bound conjectured in the AdS/CFT correspondence, posing an intriguing question regarding the applicability of the conjecture to QCD systems.

The viscosity extraction method may be extended for fully exploring the transport properties at finite density using the experimental data from high-density nuclear collisions where the baryon chemical potential is relevant. Also it would be interesting to investigate other types of transport coefficients, such as bulk viscosity and baryon diffusion coefficient.

As briefly mentioned earlier, recently there have been arguments that the QCD medium is created also in small systems such as proton-lead and deuteron-gold collisions. The relativistic hydrodynamic model turns out to be able to describe the elliptic flow of those systems fairly well [40] while a non-hydrodynamic model based on the color glass condensate can also explain the data [41]. The existence of the smallest droplet of QGP is still controversial, but may well be justified at the energy scale of UHECR. The insights obtained through the analyses of heavy ion collisions [42] would be quite useful for quantitative understanding of the cosmic ray events.

References

[1] E. Fermi, *Prog. Theor. Phys.* **5**, 570 (1950).
 [2] I. Arsene *et al.* [BRAHMS Collaboration], *Nucl. Phys. A* **757**, 1 (2005).
 [3] B. B. Back *et al.* [PHOBOS Collaboration], *Nucl. Phys. A* **757**, 28 (2005).
 [4] J. Adams *et al.* [STAR Collaboration], *Nucl. Phys. A* **757**, 102 (2005).
 [5] K. Adcox *et al.* [PHENIX Collaboration], *Nucl. Phys. A* **757**, 184 (2005).
 [6] K. Yagi, T. Hatsuda and Y. Miake, *Quark-Gluon Plasma: From Big Bang To Little Bang*, Cambridge Monographs on Particle Physics, Nuclear Physics and Cosmology (Cambridge University Press, Cambridge, England, 2005), 1

[7] A. M. Poskanzer and S. A. Voloshin, *Phys. Rev. C* **58**, 1671 (1998).
 [8] J. -Y. Ollitrault, *Phys. Rev. D* **46**, 229 (1992).
 [9] S. Z. Belenkij and L. D. Landau, *Nuovo Cim. Suppl.* **3S10**, 15 (1956) [*Usp. Fiz. Nauk* **56**, 309 (1955)].
 [10] J. D. Bjorken, *Phys. Rev. D* **27**, 140 (1983).
 [11] L. D. McLerran and R. Venugopalan, *Phys. Rev. D* **49**, 2233 (1994).
 [12] L. D. McLerran and R. Venugopalan, *Phys. Rev. D* **49**, 3352 (1994).
 [13] T. Lappi and L. McLerran, *Nucl. Phys. A* **772**, 200 (2006).
 [14] F. Cooper and G. Frye, *Phys. Rev. D* **10**, 186 (1974).
 [15] W. Israel and J. M. Stewart, *Annals Phys.* **118**, 341 (1979).
 [16] A. Monnai, *Phys. Rev. C* **86**, 014908 (2012).
 [17] G. S. Denicol, C. Gale, S. Jeon, A. Monnai, B. Schenke and C. Shen, *Phys. Rev. C* **98**, 034916 (2018).
 [18] A. Monnai, *Phys. Rev. C* **98**, 034902 (2018).
 [19] S. Borsanyi, Z. Fodor, C. Hoelbling, S. D. Katz, S. Krieg and K. K. Szabo, *Phys. Lett. B* **730**, 99 (2014).
 [20] A. Bazavov *et al.* [HotQCD Collaboration], *Phys. Rev. D* **90**, 094503 (2014).
 [21] J. M. Maldacena, *Int. J. Theor. Phys.* **38**, 1113 (1999) [*Adv. Theor. Math. Phys.* **2**, 231 (1998)].
 [22] P. Kovtun, D. T. Son and A. O. Starinets, *Phys. Rev. Lett.* **94**, 111601 (2005).
 [23] G. Denicol, A. Monnai and B. Schenke, *Phys. Rev. Lett.* **116**, 212301 (2016).
 [24] G. S. Denicol, H. Niemi, E. Molnar and D. H. Rischke, *Phys. Rev. D* **85**, 114047 (2012) Erratum: [*Phys. Rev. D* **91**, 039902 (2015)].
 [25] G. S. Denicol, S. Jeon and C. Gale, *Phys. Rev. C* **90**, 024912 (2014).
 [26] B. Schenke, S. Jeon, C. Gale, *Phys. Rev. Lett.* **106**, 042301 (2011).
 [27] A. Monnai and B. Schenke, *Phys. Lett. B* **752**, 317 (2016).
 [28] S. Jeon and J. I. Kapusta, *Phys. Rev. C* **56**, 468 (1997).
 [29] S. Borsanyi, Z. Fodor, S. D. Katz, S. Krieg, C. Ratti and K. Szabo, *JHEP* **1201**, 138 (2012).
 [30] J. Cleymans, H. Oeschler, K. Redlich and S. Wheaton, *Phys. Rev. C* **73**, 034905 (2006).
 [31] L. P. Csernai, J. I. Kapusta and L. D. McLerran, *Phys. Rev. Lett.* **97**, 152303 (2006).
 [32] P. B. Arnold, G. D. Moore and L. G. Yaffe, *JHEP* **0305**, 051 (2003).
 [33] M. Prakash, M. Prakash, R. Venugopalan and G. Welke, *Phys. Rept.* **227**, 321 (1993).
 [34] S. Ryu, J.-F. Paquet, C. Shen, G. S. Denicol, B. Schenke, S. Jeon and C. Gale, *Phys. Rev. Lett.* **115**, no. 13, 132301 (2015).
 [35] K. Okamoto and C. Nonaka, arXiv:1712.00923 [nucl-th].

- [36] B. B. Back *et al.* [PHOBOS Collaboration], Phys. Rev. Lett. **94**, 122303 (2005).
- [37] B. B. Back *et al.* [PHOBOS Collaboration], Phys. Rev. C **72**, 051901 (2005).
- [38] G. Denicol, A. Monnai, S. Ryu and B. Schenke, Nucl. Phys. A **956**, 288 (2016).
- [39] L. Adamczyk *et al.* [STAR Collaboration], Phys. Rev. C **88**, 014904 (2013).
- [40] R. D. Weller and P. Romatschke, Phys. Lett. B **774**, 351 (2017).
- [41] M. Mace, V. V. Skokov, P. Tribedy and R. Venugopalan, Phys. Rev. Lett. **121**, 052301 (2018).
- [42] T. Pierog, I. Karpenko, J. M. Katzy, E. Yatsenko and K. Werner, Phys. Rev. C **92**, 034906 (2015).